Journal of Photochemistry, 7 (1977) 123 - 139

THE PHOTOLYSIS OF SULFUR DIOXIDE IN THE PRESENCE OF FOREIGN GASES
X: EXCITATION OF SO_2 AT 3600 - 4100 Å IN THE PRESENCE OF ALLENE

NELSON KELLY and JULIAN HEICKLEN

Department of Chemistry and Center for Air Environment Studies, The Pennsylvania State University, University Park, Pa. 16802 (U.S.A.)

(Received October 6, 1976; in revised form February 10, 1977)

Summary

SO_2 was photolyzed at 25 °C and at wavelengths of 3600 - 4100 Å in the presence of allene. The quantum yields of the gas phase products C_2H_4 and CO were determined over a range of allene and SO_2 pressures as well as in the presence of CO_2 and NO. At lower pressures the quantum yield $\Phi\{C_2H_4\}$ of C_2H_4 increases with the ratio [allene]/[SO_2] to a maximum value of 0.0024. In the presence of CO_2 or NO or at the higher allene pressures $\Phi\{C_2H_4\}$ is reduced. The results can be explained in terms of all the C_2H_4 coming from the emitting triplet $SO_2(^3B_1)$. The quantum yield $\Phi\{CO\}$ of CO also increases with the ratio [allene]/[SO_2] to a maximum value of 0.026. However, the increase is very slight over a large variation in this ratio. In the presence of CO_2 or NO $\Phi\{CO\}$ is reduced, although CO_2 does not cause a very dramatic reduction. The emitting triplet as well as the non-emitting triplet are necessary to interpret $\Phi\{CO\}$. The proposed mechanism derived from our previous studies of the photo-oxidation of allene and acetylene by excited SO_2 can be used to fit the results of this study.

Introduction

The photo-oxidation of acetylene and allene by SO_2 irradiated at 3130 Å has recently been reported from this laboratory [1 - 3]. The products of these photolyses were CO and an aerosol for acetylene [4], and CO, C_2H_4 and an aerosol for allene [5]. For acetylene the reaction was shown to proceed solely through triplet states, both the emitting triplet, designated SO_2 ($^3B_1$), and a non-emitting triplet, designated SO_2^{**}, first proposed by Cehelnik *et al.* [6]. In order to test this hypothesis the photo-oxidation of acetylene by SO_2 at 3600 - 4100 Å was investigated [7]. In this wavelength region the absorption produces $SO_2(^3B_1)$ directly. Although SO_2^{**} was still found to be necessary to interpret our results, basically $SO_2(^3B_1)$ was responsible for at least 90% of the CO production in accordance with our expectations.

In the photolysis at 3130 Å of SO_2 in the presence of allene (C_3H_4) the mechanism was considerably more complex than for acetylene [3]. Not only does it appear that the emitting singlet $SO_2(^1B_1)$ as well as the two triplet states are reactive, but a quenchable excited intermediate was necessary in order to fit the results.

The mechanism which we have previously proposed for the photo-oxidation of olefins by SO_2 [1 - 5], and which was obtained from previous work in our laboratory on photo-excited SO_2 [8 - 11], correlates with the work of others. For example Wampler [12] and Wampler and Bottenheim [13] have recently shown that the $SO_2(^3B_1)$ state is very efficient in causing the *cis–trans* isomerization of substituted but-2-enes. Wampler also found that it has a very high cross section for quenching by aromatic hydrocarbons [14]. The $SO_2(^3B_1)$ state was produced both by intersystem crossing from the singlet(s) produced on absorption and by direct absorption into the triplet band. Previous to this Calvert and coworkers [15 - 18] and Timmons [19] had also presented evidence of the reactivity of $SO_2(^3B_1)$.

In addition recently many workers have needed SO_2^{**} or a state similar to it to explain their results at high pressures. Thus for example Simons *et al.* [20] needed another triplet state that is not competitively quenched by Ar, He or CH_4 to explain the production of SO ($\tilde{X}^3\Sigma^-$) in their flash photolysis of SO_2 at $\lambda > 2350$ Å. Penzhorn and Filby [21] needed a similar state to explain their high isomerization yield of *cis*-but-2-ene photosensitized by SO_2. Calvert and coworkers [22 - 24] agree that at high pressures a new state is formed but they have argued that this state only serves to produce excess $SO_2(^3B_1)$ rather than to react directly. Cox [25], in a study of the *cis*-but-2-ene isomerization by excited SO_2, obtained similar results (excess yields over those predicted by only $SO_2(^3B_1)$), but he suggested that the singlet may be reacting.

In a similar manner to the SO_2–acetylene system it would be interesting to see whether the mechanism proposed for the SO_2–allene system at 3130 Å would accommodate the results of photolysis at 3600 - 4100 Å. In this region the relative amounts of $SO_2(^3B_1)$ and SO_2^{**} that should be present are known from the previous SO_2–C_2H_2 study [7], and contributions from $SO_2(^1B_1)$ should be eliminated or greatly reduced. In order to test further the consistency of the mechanism that we have previously proposed, we have undertaken a study of the reaction of SO_2 excited at 3600 - 4100 Å with allene in the absence and in the presence of other quenching gases.

Experimental

The apparatus used in this study was identical to that used in our previous study of the SO_2–C_2H_2 system at 3600 - 4100 Å [7], except that some additional equipment was needed to measure C_2H_4. The gas handling and purification procedures for SO_2, NO and CO_2 were exactly as described before. The photolysis cell, radiation source and filter system were identical to those

used previously. The spectral distribution of the optical system as well as the procedure for matching the SO_2 absorbance to that of azomethane are described elsewhere [7].

The allene used in this study was supplied by Linde/Union Carbide. It was purified with a modified preparative gas chromatograph (Loenco Model 160 series) employing a 30 ft column of dimethyl sulfolane and was then distilled twice from — 130 °C (n-pentane slush) to — 160 °C (isopentane slush).

Since only about one-tenth as much CO was produced under similar conditions by this system as by the SO_2–C_2H_2 system, and yet we used the same analytical procedure, our experimental error was greater in this study. In order to collect sufficient CO for measurement longer photolysis times had to be used. Other than this all procedures concerning CO measurement were exactly as described previously [2, 7].

In order to measure C_2H_4 a Varian Model 1520 gas chromatograph with flame ionization detection was used. The mixture was separated by a 6 ft × ¼ in o.d. copper column packed with 60/80 mesh Chromosorb 101 maintained at 35 °C and with a flow rate of 210 cm^3 min^{-1} of helium. The amount of C_2H_4 produced was so small that it had to be transferred, using a Toepler pump, to a sample loop with a volume of approximately 10 cm^3 and injected. The SO_2 and most of the C_3H_4 were held back by a spiral trap cooled to — 160 °C (isopentane slush). The flame ionization detector was calibrated with standard samples of C_2H_4 and was checked each day by injecting a standard mixture of C_2H_4 in C_3H_4. The ratio of C_3H_4 to C_2H_4 remained constant to within 10% and the sensitivity varied from injection to injection by about 20%. This error which came from injection system irregularities as well as changes in burning of the flame from day to day is our minimum experimental error using the flame ionization detector.

The — 160 °C trap allowed us to hold back CO_2 when this was added as a quenching gas and C_2H_4 was measured. However, with NO as the quenching gas it was impossible to separate the C_2H_4 from NO by using a cooled trap. Since only small amounts were added, however, all the NO was collected with the C_2H_4 and injected into the gas chromatograph. This resulted in substantial broadening of the peaks.

Because of insufficient product, the whole sample was needed for analysis. Therefore separate experiments were done to measure CO (concentration by Toepler pump and thermistor detection) and C_2H_4 (concentration by Toepler pump and flame ionization detection).

After each experiment the cell was thoroughly pumped out, a few torr of He were added and the cell was again thoroughly pumped out. This was done twice to remove any background traces of C_2H_4. In order to keep the concentration of reactants virtually constant at their initial values, photolysis times were kept as short as possible, consistent with allowing adequate product to be collected for analysis.

Results

All experiments were carried out at 25 °C with radiation centered at 3850 Å and a full-width half-maximum of 230 Å (effective radiation from 3600 to 4100 Å). First it was verified that SO_2 excited with radiation in this region reacts with C_3H_4 to give C_2H_4. After this experiment, with the SO_2 pressure at 25 ± 3 Torr, the C_3H_4 pressure was varied from 45 mTorr to 27 Torr. Photolysis times were varied by a factor of 2 from 4000 to 8000 s with no systematic variation in $\Phi\{C_2H_4\}$ within the experimental error. The absorbed light intensity I_a for these runs was 0.028 ± 0.003 mTorr min^{-1}. The data are shown in Fig. 1.

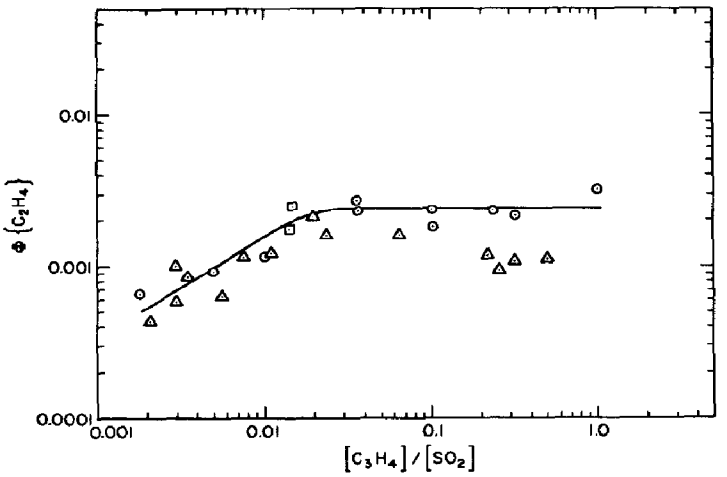

Fig. 1. Log–log plots of $\Phi\{C_2H_4\}$ *vs.* $[C_3H_4]/[SO_2]$ for various SO_2 pressures (in Torr): ○ 25 ± 3.0, □ 40, △ 100 ± 5. The curve is drawn to fit all the data at low pressures of $[C_3H_4]$ and the $[SO_2]$ = 25 Torr data at higher pressures of $[C_3H_4]$.

Another series of experiments was done with an SO_2 pressure of 100 ± 5 Torr, $[C_3H_4]$ from 0.214 to 50 Torr and I_a = 0.114 ± 0.003 mTorr min^{-1}. Again the photolysis times were varied by a factor of 2 and no systematic variation was noted in $\Phi\{C_2H_4\}$. Two runs were also done with an SO_2 pressure of 39 Torr, 0.58 Torr of C_3H_4 and I_a = 0.045 mTorr min^{-1}. The data from these runs are also plotted in Fig. 1.

At low values of $[C_3H_4]/[SO_2]$, $\Phi\{C_2H_4\}$ increases with the ratio to an upper limiting value of 0.0024 at $[C_3H_4]/[SO_2] \approx 0.02$. At 25 Torr of SO_2, $\Phi\{C_2H_4\}$ remains at 0.0024 as $[C_3H_4]/[SO_2]$ is increased further. However, at 100 Torr of SO_2, $\Phi\{C_2H_4\}$ falls to 0.001 as $[C_3H_4]/[SO_2]$ increases to 0.5.

With $[SO_2]$ = 39.5 ± 0.4 Torr, $[C_3H_4]$ = 0.59 ± 0.01 Torr, and I_a = 0.045 ± 0.001 mTorr min^{-1}, up to 470 Torr of CO_2 was added. A plot of $\Phi\{C_2H_4\}^{-1}$ *versus* $[CO_2]$ is shown in Fig. 2. The plot is linear and the least-squares line gives a slope of 4.22 $Torr^{-1}$ and an intercept of 639.

With NO added, the quenching was marked and large amounts of NO were not needed. With $[SO_2]$ = 39.7 ± 0.5 Torr, $[C_3H_4]$ = 0.58 ± 0.02 Torr,

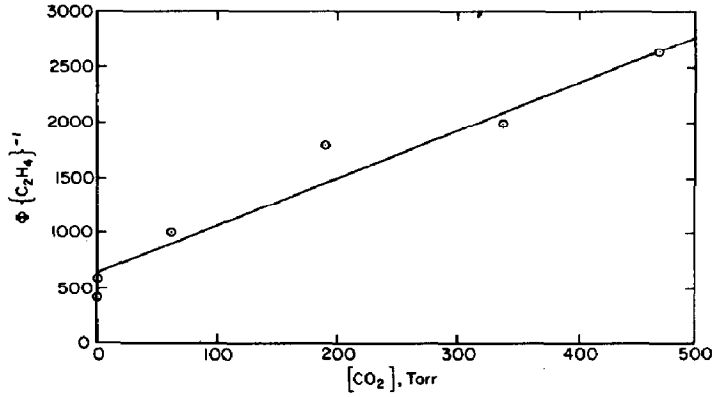

Fig. 2. Plot of $\Phi\{C_2H_4\}^{-1}$ *vs.* $[CO_2]$ for $[SO_2]$ = 39.5 ± 0.4 Torr, $[C_3H_4]$ = 0.59 ± 0.02 Torr, I_a = 0.045 ± 0.001 mTorr min^{-1}. The line drawn is the least-squares fit to the data points.

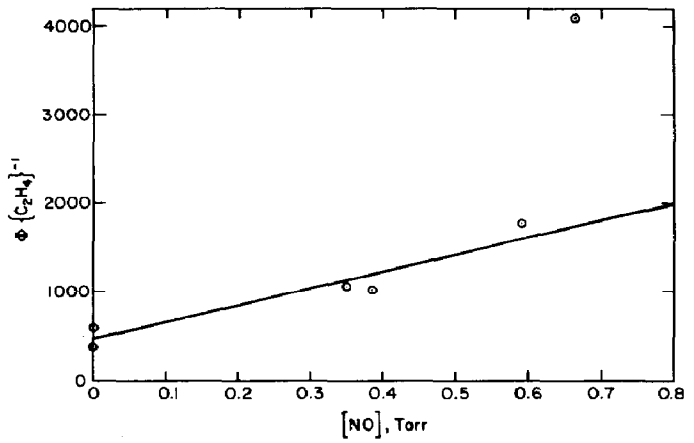

Fig. 3. Plot of $\Phi\{C_2H_4\}^{-1}$ *vs.* [NO] for $[SO_2]$ = 39.7 ± 0.5 Torr, $[C_3H_4]$ = 0.58 ± 0.02 Torr, I_a = 0.045 ± 0.001 mTorr min^{-1}. The line drawn is the least-squares fit to the data points excluding the point at highest [NO].

and I_a = 0.045 ± 0.001 mTorr min^{-1} up to 0.655 Torr of NO was added. The results are shown in Fig. 3. Because NO is not easily separated from C_2H_4, all the NO was collected with the C_2H_4 and injected into the gas chromatograph. This broadened the C_2H_4 peaks and the data are very approximate. Nevertheless, except for one data point, the plot of $\Phi\{C_2H_4\}^{-1}$ *versus* [NO] can be represented by a straight line with a slope of 1923 $Torr^{-1}$ and an intercept of 445.

In a similar manner it was verified that CO was produced upon photolysis. Five series of runs were made under the conditions given in Table 1.

The quantum yields $\Phi\{CO\}$ of CO formation are given in Fig. 4, with the data at $[SO_2]$ = 25 Torr and $[SO_2]$ = 35 Torr being combined. With 25 Torr of SO_2 and 2.9 Torr of allene, the photolysis time was varied from 2400 to 5400 s. There was no systematic variation in the quantum yields, indicating

TABLE 1

$[SO_2]$ (Torr)	$[C_3H_4]$ (Torr)	I_a (mTorr min^{-1})
12 - 14	0.097 - 0.983	0.015 ± 0.001
20 - 30	0.048 - 250	0.028 ± 0.005
35.1	0.126	0.040
70 - 100	0.164 - 28.5	0.100 ± 0.014
196 - 204	0.422 - 34.1	0.23 ± 0.020

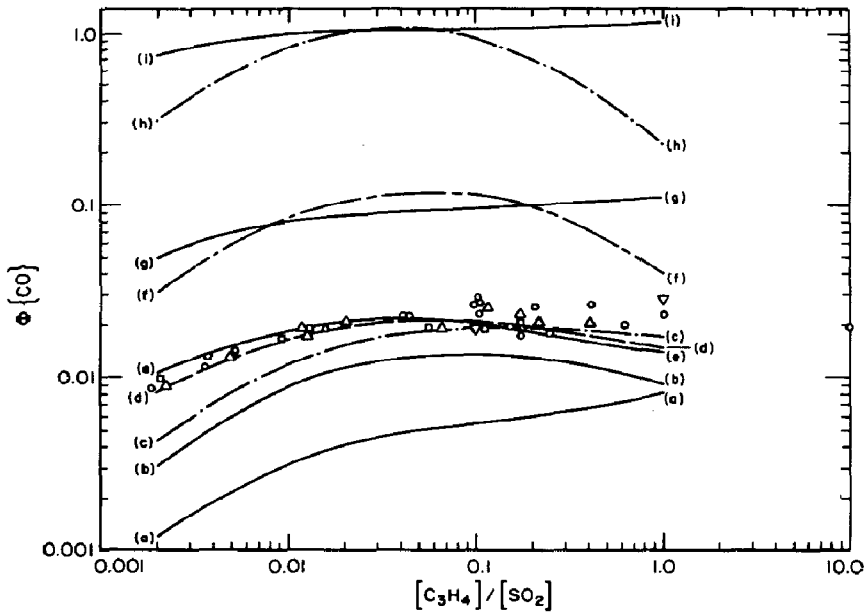

Fig. 4. Plots of $\Phi\{CO\}$ *vs.* $[C_3H_4]/[SO_2]$. The data points are for the following pressures of SO_2 (in Torr): ▽ 12.5 ± 1.0, ○ 28 ± 8.0, △ 85 ± 13.0, □ 200 ± 4.0. All the curves are computed using the rate coefficients listed in Table 2. Curves (b), (f) and (h) are $\Phi^3\{CO\}$ for $[SO_2]$ = 25, 100 and 200 Torr respectively with curves (f) and (h) shifted by factors of 10 and 100 respectively. Curves (a), (g) and (i) are $\Phi^{**}\{CO\}$ for $[SO_2]$ = 25, 100 and 200 Torr respectively with curves (g) and (i) shifted by factors of 10 and 100 respectively. Curves (c), (d) and (e) are $\Phi\{CO\}$ for $[SO_2]$ = 25, 100 and 200 Torr respectively.

that CO is an initial product and light scattering by the aerosol is not important under our conditions. The same can be said, although not as conclusively since the experimental scatter is greater, for $\Phi\{C_2H_4\}$.

In Fig. 4 $\Phi\{CO\}$ is essentially independent of the SO_2 pressure and shows a mild dependence on $[C_3H_4]/[SO_2]$, rising from 0.009 at $[C_3H_4]/[SO_2]$ = 0.002 to about 0.025 at $[C_3H_4]/[SO_2]$ = 1.0.

$\Phi\{CO\}$ was obtained in two series of runs in which CO_2 was added. In one series with $[SO_2]$ = 12.5 ± 0.5 Torr, $[C_3H_4]$ = 1.18 ± 0.03 Torr, and I_a = 0.0145 ± 0.005 mTorr min^{-1}, up to 368 Torr of CO_2 was added. In the second series with $[SO_2]$ = 98.6 ± 1.0 Torr, $[C_3H_4]$ = 1.17 ± 0.04 Torr, and I_a = 0.113 ± 0.002 mTorr min^{-1}, up to 476 Torr of CO_2 was added. These results

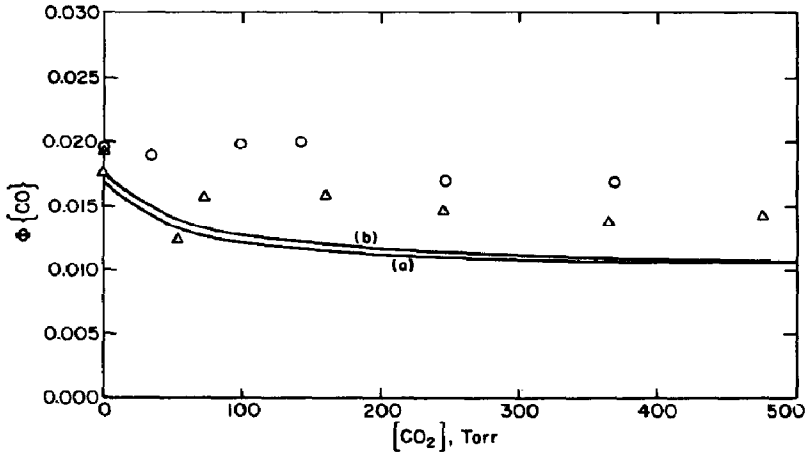

Fig. 5. Plots of $\Phi\{CO\}$ *vs.* $[CO_2]$. The curves are computed using the rate coefficients listed in Table 2. For curve (a) $[SO_2]$ = 12.5 ± 0.04 Torr and $[C_3H_4]$ = 1.17 ± 0.02 Torr. For curve (b) $[SO_2]$ = 98.6 ± 1.0 Torr and $[C_3H_4]$ = 1.17 ± 0.04 Torr. The data points are (in Torr): ○ $[SO_2]$ = 12.5 ± 0.4, $[C_3H_4]$ = 1.17 ± 0.02; △ $[SO_2]$ = 98.6 ± 1.0, $[C_3H_4]$ = 1.17 ± 0.04.

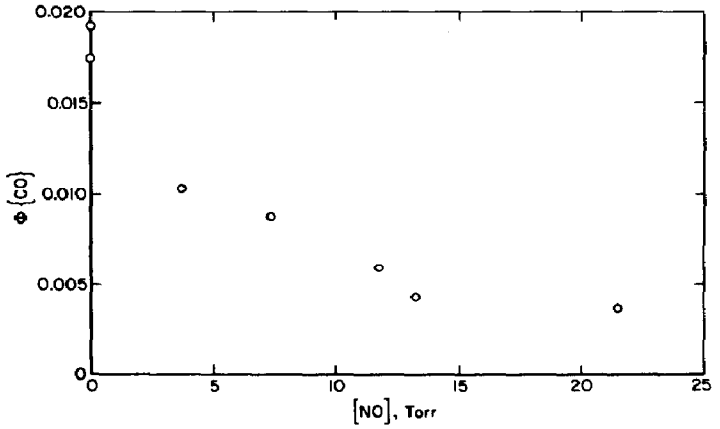

Fig. 6. Plot of $\Phi\{CO\}$ *vs.* $[NO]^{-1}$ for $[SO_2]$ = 100 ± 3.0 Torr, $[C_3H_4]$ = 1.18 ± 0.03 Torr, I_a = 0.115 ± 0.004 mTorr min^{-1}.

are shown in Fig. 5. In both series $\Phi\{CO\}$ drops slightly from about 0.018 in the absence of CO_2 to about 0.015 in the presence of 400 Torr CO_2. However, the drop is so slight that it lies within the uncertainty of the measurements.

Up to 21.5 Torr NO was added with the SO_2 pressure at 100 ± 3 Torr, the C_3H_4 pressure at 1.18 ± 0.03 Torr, and I_a = 0.116 ± 0.003 mTorr min^{-1}. Figure 6 shows a plot of $\Phi\{CO\}$ *versus* [NO]. Reduction of $\Phi\{CO\}$ from about 0.018 in the absence of NO to about 0.004 in the presence of about 20 Torr NO occurs readily.

Blank runs were done with large pressures of each of the gases and there was no background CO or C_2H_4. Also 600 Torr of SO_2 was photolyzed alone for 2 h with no CO or C_2H_4 being produced. In addition a mixture of 100 Torr

of SO_2 and 5 Torr of C_3H_4 was allowed to stand overnight. No dark reaction to produce CO or C_2H_4 was observed. However, background C_2H_4 could always be found in the system using the Toepler pump and presumably this came from aerosol or other impurities which decompose in the Toepler pump. By cleaning the Toepler pump periodically (including the mercury) and by passing helium through it before each analysis this background correction was kept negligible. With CO analysis this problem was not encountered.

Discussion

The major conclusions that can be drawn from this study can be summarized as follows.

(1) SO_2 photo-excited at 3600 - 4100 Å reacts with C_3H_4 to produce both C_2H_4 and CO.

(2) The chemically reactive states are triplets, since both CO and C_2H_4 production are readily eliminated in the presence of relatively small amounts of NO, a known efficient triplet quencher.

(3) $\Phi\{C_2H_4\}$ depends on the pressures of SO_2 and C_3H_4, as well as on CO_2 if it is added.

(4) $\Phi\{CO\}$ is somewhat dependent on $[C_3H_4]/[SO_2]$, but is otherwise not very dependent on the SO_2 pressure or the CO_2 pressure if CO_2 is added.

The mechanism chosen to fit our results is similar to that used in the study of SO_2–C_3H_4 at 3130 Å, except that now $\tilde{S}O_2(^1B_1)$ is absent and SO_2^* is produced at some fraction β of the absorbed intensity I_a. The entire mechanism is

$SO_2 + h\nu$	→ $^3SO_2$	rate = $(1-\beta)I_a$	
	→ SO_2^*	rate = βI_a	
$^3SO_2$	→ $SO_2 + h\nu_p$		(1)
$^3SO_2 + C_3H_4$	→ I		(2a)
	→ $SO_2 + C_3H_4$		(2b)
I	→ $CO + C_2H_4$ (+SO)		(3a)
	→ CO (+C_2H_4SO)		(3b)
$I + C_3H_4$	→ not CO or C_2H_4		(4a)
I + M	→ not CO or C_2H_4		(4b)
$^3SO_2 + SO_2$	→ $2SO_2$		(5)
$^3SO_2$ + M	→ SO_2 + M		(6)
SO_2^*	→ removal		(7)
$SO_2^* + C_3H_4$	→ $SO_2^{**} + C_3H_4$		(8a)

	→	$SO_2 + C_3H_4$	(8b)
$SO_2^* + M$	→	$SO_2^{**} + M$	(9a)
	→	$SO_2 + M$	(9b)
SO_2^{**}	→	SO_2	(14)
$SO_2^{**} + C_3H_4$	→	CO	(15a)
	→	removal of SO_2^{**}	(15b)
$SO_2^{**} + NO$	→	removal of SO_2^{**}	(16)

For comparison purposes we have used the same reaction numbers as Partymiller *et al.* [3]. We abbreviate the emitting triplet $SO_2(^3B_1)$ as $^3SO_2$, an excited state formed directly on absorption in this study. The SO_2^* state is a singlet and it is also produced on absorption. As was found from the photolysis of SO_2 in the presence of acetylene at 3600 - 4100 Å, there is also a small fraction of SO_2^* formed with radiation at this wavelength.

The SO_2^{**} state is the non-emitting triplet which is not quenched by SO_2 and leads to CO formation at least part of the time by reaction with allene. The symbol I represents an intermediate, postulated by Partymiller *et al.* [3], formed when $^3SO_2$ reacts with allene. It was introduced to fit the quenching data which otherwise did not fit the known quenching constants for $^3SO_2$ by SO_2, CO_2, NO and H_2O.

Reaction (3), which may or may not be a fundamental reaction, is written as such to show two parallel paths, one of which produces CO while the other produces both CO and C_2H_4. The intermediate may also be quenched by SO_2, CO_2 and NO not to give CO or C_2H_4. In reaction (15) a similar situation applies where the SO_2^{**}–C_3H_4 adduct has two possible fates, one of which produces CO.

A detailed analysis of the steady state expressions reveals that

$$\Phi\{C_2H_4\} = \frac{(1-\beta)k_{2a}k_{3a}[C_3H_4]}{(k_2[C_3H_4] + k_5[SO_2] + k_6[M])(k_3 + k_{4a}[C_3H_4] + k_{4b}[M])} \quad \text{(I)}$$

and similarly

$$\Phi\{CO\} = \frac{(1-\beta)k_{2a}k_3[C_3H_4]}{(k_2[C_3H_4] + k_5[SO_2] + k_6[M])(k_3 + k_{4a}[C_3H_4] + k_{4b}[M])} + \frac{\beta k_{15a}[C_3H_4](k_{8a}[C_3H_4] + k_{9a}[M])}{(k_7 + k_8[C_3H_4] + k_9[M])(k_{14} + k_{15}[C_3H_4] + k_{16}[NO])} \quad \text{(II)}$$

In the above two equations M represents SO_2, CO_2 or NO except in reaction (6) where it cannot be SO_2. In eqn. (I) $\Phi\{C_2H_4\} = \Phi^3\{C_2H_4\}$; *i.e.* all the ethylene comes from the emitting triplet as found by Partymiller *et al.* [3]. The first term on the right-hand side in eqn. (II) is merely $(k_3/k_{3a})\Phi\{C_2H_4\}$ and is the quantum yield of CO from the emitting triplet. We shall call this $\Phi^3\{CO\}$. The second term on the right-hand side in eqn. (II) represents the contribution of SO_2^{**} to $\Phi\{CO\}$. It will be called $\Phi^{**}\{CO\}$.

TABLE 2

Summary of rate coefficient information

Ratio	Value	Units	M	Reference
k_2/k_5	124	None	–	This work
	90	None	–	Partymiller *et al.* [3]
k_{2a}/k_2	0.0167	None	C_3H_4	Partymiller *et al.* [3]
k_{3a}/k_3	0.14	None	C_3H_4	This work
k_{4a}/k_3	0.029	$Torr^{-1}$	C_3H_4	This work
	0.02	$Torr^{-1}$	C_3H_4	Partymiller *et al.* [3]
k_{4b}/k_3	0.012	$Torr^{-1}$	CO_2	This work
	0.02	$Torr^{-1}$	CO_2	Partymiller *et al.* [3]
k_6/k_5	~250	None	NO	This work
	80	None	NO	Kelly *et al.* [2]
	80	None	NO	Partymiller *et al.* [3]
	74	None	NO	Kelly *et al.* [7]
	64	None	NO	Mettee [26]
	~100	None	NO	Stockburger *et al.* [10]
	190	None	NO	Sidebottom *et al.* [27]
	200	None	NO	Penzhorn and Gusten [28]
k_6/k_5	0.42	None	CO_2	Kelly *et al.* [2]
	0.55	None	CO_2	Stockburger *et al.* [10]
	0.55	None	CO_2	Partymiller *et al.* [3]
	0.31	None	CO_2	Mettee [26]
	0.29	None	CO_2	Sidebottom *et al.* [27]
k_7/k_9	70.6	Torr	CO_2	Kelly *et al.* [7]
k_7/k_9	~32	Torr	SO_2	Kelly *et al.* [7]
k_7/k_8	22	Torr	C_3H_4	Partymiller *et al.* [3]
k_{9a}/k_9	~1	None	SO_2	Kelly *et al.* [7]
k_{9a}/k_9	~1	None	CO_2	This work
k_{8a}/k_8	~1	None	C_3H_4	This work
k_{14}/k_{15}	0.159	Torr	C_3H_4	This work
	0.255	Torr	C_3H_4	Partymiller *et al.* [3]
k_{14}/k_{16}	0.164	Torr	NO	Kelly *et al.* [2]
	0.17	Torr	NO	Partymiller *et al.* [3]
	0.34	Torr	NO	Cehelnik *et al.* [8]
k_{15a}/k_{15}	0.25	None	C_3H_4	This work
β	> 0.05	None	–	Kelly *et al.* [7]

TABLE 3

Average quantum yields for C_2H_4*

$[SO_2]/[C_3H_4]$	$\Phi\{C_2H_4\}$
50	0.0024
67	0.00195
100	0.00153
125	0.00132
200	0.00096
333	0.00070
500	0.00054

*Obtained from the curve in Fig. 1.

Analysis of C_2H_4 data

In the absence of foreign gases eqn. (I) can be rearranged to

$$\Phi\{C_2H_4\}^{-1} = \frac{k_2}{(1-\beta)k_{2a}}\frac{k_3}{k_{3a}}\left(1+\frac{k_5}{k_2}\frac{[SO_2]}{[C_3H_4]}\right)\left(1+\frac{k_{4a}[C_3H_4]}{k_3}+\frac{k_{4b}[SO_2]}{k_3}\right) \quad \text{(III)}$$

Using the rate coefficient ratios of Partymiller *et al.* [3] listed in Table 2 along with their finding that $k_{4b}/k_3 \ll 0.02$ and the finding of Kelly *et al.* [7] that $1-\beta \sim 1$, we find that 0.0167 should be the upper limiting value for $\Phi\{C_2H_4\}$. From Fig. 1 we see that in fact the upper limiting value is about 0.0024. Thus the efficiency with which reaction (3) forms C_2H_4 must be much less at 3600 - 4100 Å than that at 3130 Å. If k_{3a}/k_3 is approximately 0.14 this would be the case, while at 3130 Å this ratio was found to be 0.5 [3]. Although the data in Fig. 1 are scattered we can draw a smooth curve that fits all the points at low values of $[C_3H_4]/[SO_2]$. The data are not good enough to see any dependence other than on the ratio at low $[C_3H_4]/[SO_2]$. The curve drawn represents average quantum yields (Table 3), and from eqn. (I) we may plot the reciprocals of these average quantum yields *versus* $[SO_2]/[C_3H_4]$ to obtain k_2/k_5 as the ratio of intercept to slope (Fig. 7). An

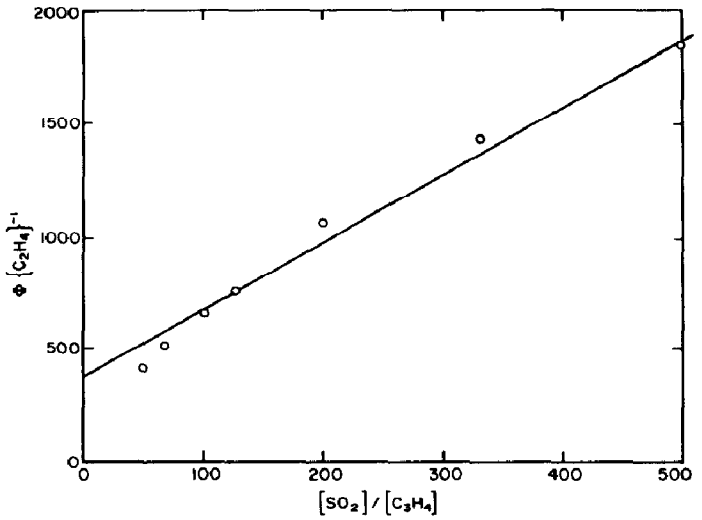

Fig. 7. Plot of $\Phi\{C_2H_4\}^{-1}$ *vs.* $[SO_2]/[C_3H_4]$. The points used are not data points and are obtained from the smooth curve drawn in Fig. 1 and listed in Table 3.

implicit assumption in using these average quantum yields has been that $1 + k_{4a}[C_3H_4]/k_3 + k_{4b}[SO_2]/k_3$ is about 1 for $[SO_2]$ = 25 - 100 Torr and $[C_3H_4]/[SO_2]$ = 0.002 - 0.02. Since Partymiller *et al.* [3] report k_{4a}/k_3 to be 0.02 and their data did not require SO_2 to act as M in reaction (4b), this assumption seems to be valid. The ratio of intercept to slope in Fig. 7 gives a value of k_2/k_5 = 124, in reasonable agreement with the value of 90 found by Partymiller *et al.* [3]. Both values are listed in Table 2.

We can obtain an estimate from our data of k_{4a}/k_3 and k_{4b}/k_3 from a plot of $\Phi\{C_2H_4\}^{-1}(1 + k_5[SO_2]/k_2[C_3H_4])^{-1}$ *versus* $[C_3H_4]$ for the points where $[SO_2]$ = 100 Torr. That is, from eqn. (I),

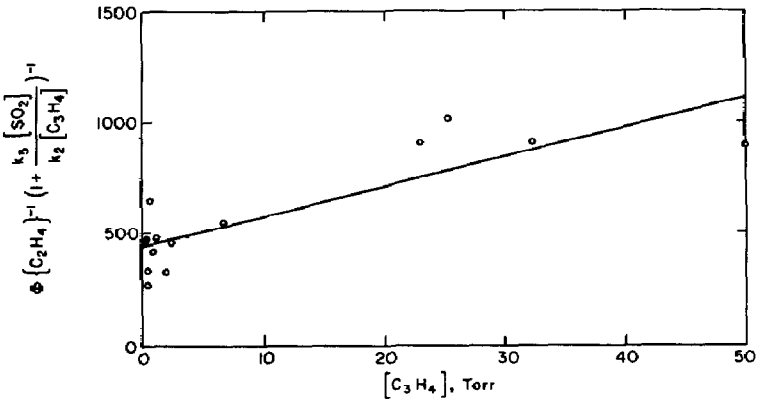

Fig. 8. Plot of $\Phi\{C_2H_4\}^{-1}\left(1 + \frac{k_5}{k_2}\frac{[SO_2]}{[C_3H_4]}\right)^{-1}$ *vs.* $[C_3H_4]$ for $[SO_2] = 100 \pm 5$ Torr.

$$\left(1 + \frac{k_5[SO_2]}{k_2[C_3H_4]}\right)^{-1} \Phi\{C_2H_4\}^{-1} = \frac{1}{1-\beta}\frac{k_2}{k_{2a}}\frac{k_3}{k_{3a}}\left(1 + \frac{k_{4a}}{k_3}[C_3H_4] + \frac{k_{4b}}{k_3}[SO_2]\right) \quad \text{(IV)}$$

Figure 8 shows a plot of the left-hand side of eqn. (IV) *versus* $[C_3H_4]$. Although the data are scattered we draw the best line and obtain a slope and intercept of 13.1 and 448 respectively. From the slope and with $k_2k_3/(1-\beta)\,k_{2a}k_{3a} \sim 450$ from the rate constant ratios listed in Table 2 we obtain $k_{4a}/k_3 = 0.029$, with an experimental uncertainty of about ± 30%. This is in good agreement with the value of 0.02 obtained by Partymiller *et al.* [3]. From the intercept of Fig. 8 we obtain $k_{4b}/k_3 \sim 0$; that is, there does not seem to be any quenching of the intermediate by 100 Torr SO_2. Partymiller *et al.* [3] also discovered this, although they did not use such high SO_2 pressures.

With CO_2 added as a quenching gas we observe a strong quenching of C_2H_4 production. In order to evaluate the quenching of the intermediate by CO_2 we may rearrange eqn. (I) to

$$\Phi\{C_2H_4\}^{-1}\left(1 + \frac{k_5}{k_2}\frac{[SO_2]}{[C_3H_4]} + \frac{k_6}{k_2}\frac{[CO_2]}{[C_3H_4]}\right) = \frac{k_2k_3}{(1-\beta)k_{2a}k_{3a}}\left(1 + \frac{k_{4a}}{k_3}[C_3H_4] + \frac{k_{4b}}{k_3}[CO_2]\right) \quad \text{(V)}$$

From the data in Fig. 2 and the rate coefficients already evaluated the left-hand side of eqn. (V) can be evaluated. It is plotted against $[CO_2]$ in Fig. 9. A straight line is forced through the data. From the slope of this line, 0.534 $Torr^{-1}$, we may evaluate k_{4b}/k_3 to be 0.0012 $Torr^{-1}$ with error limits of a factor of 2. The reason for these large error limits is that, at 470 Torr of CO_2, $\Phi\{C_2H_4\}$ is so near zero that there is a very large error in measuring this

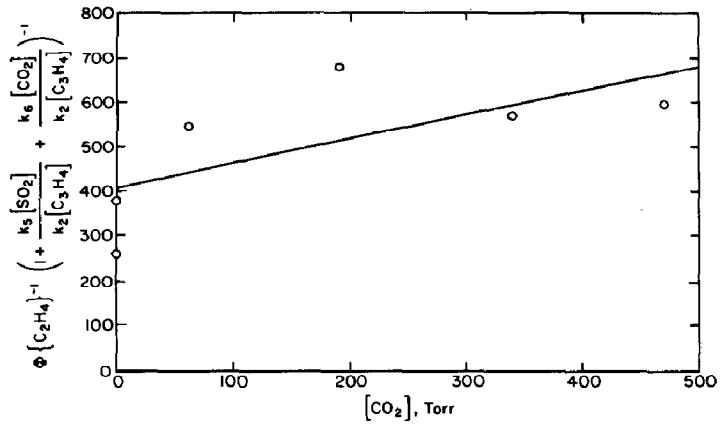

Fig. 9. Plot of $\Phi\{C_2H_4\}^{-1}$ *vs.* $\left(1+\frac{k_5}{k_2}\frac{[SO_2]}{[C_3H_4]}+\frac{k_6}{k_2}\frac{[CO_2]}{[C_3H_4]}\right)^{-1}$ for $[SO_2]$ = 39.5 ± 0.4 Torr, $[C_3H_4]$ = 0.59 ± 0.02 Torr.

amount of product. Any slight background C_2H_4 or slight amount of C_2H_4 from other states would cause non-linearity of this plot.

The C_2H_4 formation is strongly quenched by NO because it is a strong triplet state scavenger. Therefore the NO pressure used was always low enough for quenching of the intermediate I by NO to be unimportant. The rate law for $\Phi\{C_2H_4\}$ becomes

$$\Phi\{C_2H_4\}^{-1}=\frac{1}{1-\beta}\frac{k_2}{k_{2a}}\frac{k_3}{k_{3a}}\left(1+\frac{k_5[SO_2]}{k_2[C_3H_4]}+\frac{k_6[NO]}{k_2[C_3H_4]}\right)\times$$
$$\times\left(1+\frac{k_{4a}[C_3H_4]}{k_3}+\frac{k_{4b}[SO_2]}{k_3}\right) \qquad \text{(VI)}$$

Figure 3 is a plot of $\Phi\{C_2H_4\}^{-1}$ *versus* $[NO]$. The ratio of slope to intercept gives 4.32. Since $[C_3H_4]$ = 0.58 Torr, $k_6/k_2 = 2.51$. Now $k_2/k_5 \sim 100$ (see Table 2), so that $k_6/k_5 \approx 251$ from this study. This is considerably larger than the values of 64 - 100 obtained in some studies [2, 7, 26], but in line with values of 190 - 200 obtained in other studies [27, 28]. However, the error limits are so large on our value that it can be considered consistent with all the studies and cannot be used to differentiate between them.

Analysis of CO data

In the absence of foreign gases and knowing $\Phi^3\{CO\}$ from the previously determined $\Phi^3\{C_2H_4\}$ we may compute $\Phi^{**}\{CO\}$:

$$\Phi^{**}\{CO\}\equiv\Phi\{CO\}-\Phi^3\{CO\}=\frac{\beta k_{15a}[C_3H_4]\,(k_{8a}[C_3H_4]+k_{9a}[SO_2])}{(k_7+k_8[C_3H_4]+k_9[SO_2])\,(k_{14}+k_{15}[C_3H_4])} \qquad \text{(VII)}$$

For the runs where SO_2 is 85 and 200 Torr and $[C_3H_4] < 2.5$ Torr reaction (8) is negligible and eqn. (VII) can be rearranged to

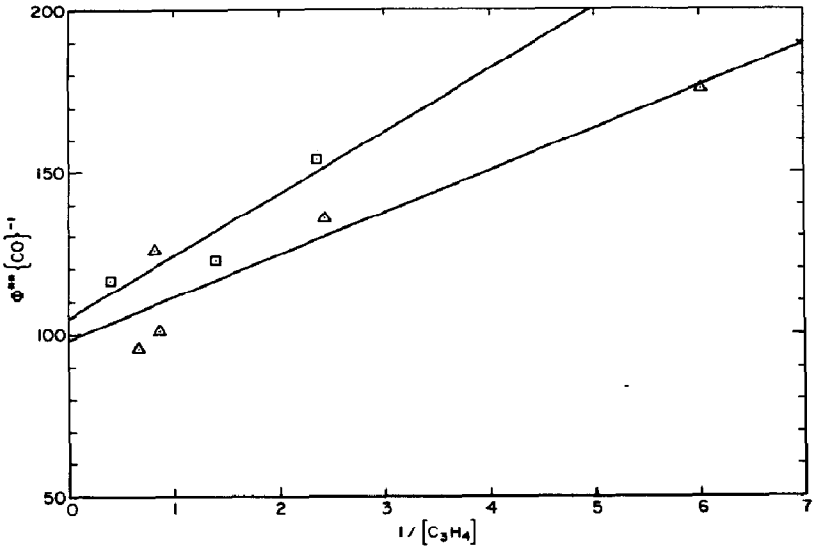

Fig. 10. Plot of $\Phi^{**}\{CO\}^{-1}$ *vs.* $1/[C_3H_4]$. The pressures of $[SO_2]$ are: △ $[SO_2] = 85 \pm 13.0$ Torr, □ $[SO_2] = 200 \pm 4.0$ Torr. $\Phi^{**}\{CO\}$ was calculated as the difference between $\Phi\{CO\}$ (from data points of Fig. 4 for these SO_2 pressures) and $\Phi^3\{CO\}$ which can be calculated using the rate coefficients of Table 2.

$$\Phi^{**}\{CO\}^{-1} = \frac{k_{15}}{\beta k_{15a}} \frac{k_7 + k_9[SO_2]}{k_{9a}[SO_2]} \left(1 + \frac{k_{14}}{k_{15}[C_3H_4]}\right) \qquad \text{(VIII)}$$

In Fig. 10 are shown plots of $\Phi^{**}\{CO\}^{-1}$ *versus* $1/[C_3H_4]$ for the two SO_2 pressures of 85 ± 13 Torr and 200 ± 4 Torr. The ratio of slope to intercept for $[SO_2]$ = 200 and 85 Torr are 0.183 and 0.135 Torr respectively. A simple average gives $k_{14}/k_{15} = 0.159$ Torr in reasonable agreement with the value of 0.255 found by Partymiller *et al.* [3]. From the intercept of about 100 of these two plots in Fig. 10 we may make an estimate of $\beta k_{15a}/k_{15}$. If we use the values of $k_7/k_9 \sim 32$ Torr and $k_{9a}/k_9 \sim 1$ as found by Kelly *et al.* [7], we obtain $\beta k_{15a}/k_{15} = 0.0139$ and 0.011 for SO_2 pressures of 85 and 200 Torr respectively. The average, 0.0125, along with $\beta \sim 0.05$ gives $k_{15a}/k_{15} = 0.25$. Partymiller *et al.* [3] knew that there had to be physical quenching of SO_2^{**} by allene and in fact that it had to occur about four times as often as with acetylene. However, they were not able to evaluate it from their data. We may now use the evaluated rate constants to predict $\Phi\{CO\}$ and the curves drawn in Fig. 4 are computed in this way. Only one additional assumption needed to be made and that is $k_{8a}/k_8 \sim 1$ since this rate constant was not evaluated and we could not evaluate it on the basis of our data.

In Fig. 4 curves (d), (e) and (f) show plots of $\Phi\{CO\}$ for $[SO_2]$ = 25, 100 and 200 Torr respectively. For $[SO_2]$ = 25 Torr the fit is not very good. There are two possible reasons for this. First there could be some CO coming from the emitting singlet. At 25 Torr of SO_2 over half of the SO_2^* is decaying by a unimolecular process to produce $^1SO_2$. At the higher SO_2 pressures this amount would be less and so qualitatively the incorporation of $^1SO_2$ should

help to explain the discrepancy. Also, however, very small amounts of products were collected in these runs at low SO_2 and C_3H_4 pressures and the experimental error is greatest here. Therefore we have not included the $^1SO_2$ contribution in our mechanism.

When CO_2 is added as a quenching gas with the SO_2 pressure at 12 Torr and an allene pressure of 1.17 Torr we may evaluate $\Phi^3\{CO\}$ from the already known rate constants. In order to evaluate $\Phi^{**}\{CO\}$ we may use $k_2/k_9 \sim 70.6$ Torr obtained by Kelly *et al.* [7] and assume that $k_{9a}/k_9 \sim 1$ for CO_2 as it is for SO_2. If $\Phi\{CO\}$ is calculated in this manner we obtain the curves shown in Fig. 5 for the SO_2 and C_3H_4 pressures shown. For the runs at 100 Torr of SO_2 the fit is good, while for 12.5 Torr of SO_2 it is only fair. In both cases the predicted curve is consistently low. Part of the reason for this could be that our estimate of k_{4b}/k_3 for CO_2 is high, *i.e.* CO_2 quenching of the intermediate is not as important as was estimated from the treatment of the ethylene data. For the runs at 12.5 Torr of SO_2 of course the experimental error is very great, while with 100 Torr of SO_2, where eight times as much product was collected in the same amount of time, the precision is greater.

When NO is the quenching gas, its pressure is low and it makes no contribution to the quenching of SO_2^* via reaction (9). Thus eqn. (II) can be rearranged to

$$\Phi^{**}\{CO\}^{-1} \equiv (\Phi\{CO\} - \Phi^3\{CO\})^{-1} = \frac{1}{\beta}\frac{k_{15}}{k_{15a}}\frac{k_7 + k_8[C_3H_4] + k_9[M]}{k_{7a}[C_3H_4] + k_{9a}[M]} \times$$
$$\times \left(1 + \frac{k_{14}}{k_{15}[C_3H_4]} + \frac{k_{16}[NO]}{k_{15}[C_3H_4]}\right) \qquad \text{(IX)}$$

and $\Phi^3\{CO\}$ is computed from the rate coefficients in Table 2 with $k_6/k_5 = 80$ for NO. Then $\Phi^{**}\{CO\}^{-1}$ can be computed and it is plotted against [NO] in Fig. 11. The ratio of slope to intercept, 0.133 $Torr^{-1}$, can be equated to

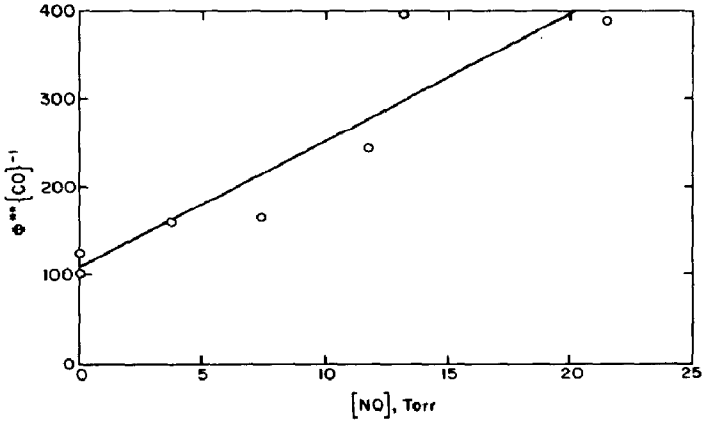

Fig. 11. Plot of $\Phi^{**}\{CO\}^{-1}$ *vs.* [NO] for $[SO_2] = 100 \pm 3$ Torr, $[C_3H_4] = 1.18 \pm 0.03$ Torr where $\Phi^{**}\{CO\}$ was calculated as the difference of $\Phi\{CO\}$ (from data points of Fig. 6) and $\Phi^3\{CO\}$ which was calculated using the rate coefficients in Table 2 with $k_6/k_5 = 80$ for NO.

$k_{16}/(k_{14} + k_{15}[C_3H_4])$. Since $k_{14}/k_{15} = 0.159$ Torr and $[C_3H_4] = 1.18$ Torr, $k_{14}/k_{16} = 0.89$. This is very much higher than that found by others (see Table 2) and indicates that some other processes must be occurring. Perhaps these involve the emitting singlet which is not readily quenched by NO or the third triplet $SO_2^{\ddagger}$ previously incorporated to account for excess product yields [2,9].

Conclusion

The data obtained from this study are accommodated by the previous mechanisms proposed from this laboratory. As in the SO_2–C_2H_2 system at 3600 - 4100 Å, the SO_2^{**} state is needed to explain some of the CO at high pressures. We feel that the combination of all of our studies leads to a consistent, although not complete, picture of the SO_2–acetylene and SO_2–allene systems.

Acknowledgments

We wish to thank Kenneth Partymiller for helpful discussions, and Dr. F. B. Wampler for access to his work prior to publication. This work was supported by the Center for Air Environment Studies at The Pennsylvania State University for which we are grateful.

References

1 M. Luria and J. Heicklen, Can. J. Chem., 52 (1974) 3451.
2 N. A. Kelly, J. F. Meagher and J. Heicklen, J. Photochem., 5 (1976) 355.
3 K. Partymiller, J. F. Meagher and J. Heicklen, J. Photochem., 6 (1977) 405.
4 M. Luria, R. G. de Pena, K. J. Olszyna and J. Heicklen, J. Phys. Chem., 78 (1974) 325.
5 M. Luria, K. J. Olszyna, R. G. de Pena and J. Heicklen, J. Aerosol Sci., 5 (1974) 435.
6 E. Cehelnik, C. W. Spicer and J. Heicklen, J. Am. Chem. Soc., 93 (1971) 5371.
7 N. A. Kelly, J. F. Meagher and J. Heicklen, J. Photochem., 6 (1977) 157.
8 E. Cehelnik, J. Heicklen, S. Braslavsky, L. Stockburger III and E. Mathias, J. Photochem., 2 (1973) 31.
9 E. M. Fatta, E. Mathias, J. Heicklen, L. Stockburger III and S. Braslavsky, J. Photochem., 2 (1973) 119.
10 L. Stockburger III, S. Braslavsky and J. Heicklen, J. Photochem., 2 (1973) 15.
11 S. Braslavsky and J. Heicklen, J. Am. Chem. Soc., 94 (1972) 4864.
12 F. B. Wampler, Int. J. Chem. Kinet., 8 (1976) 687.
13 F. B. Wampler and J. W. Bottenheim, Int. J. Chem. Kinet., 8 (1976) 585.
14 F. B. Wampler, J. Environ. Sci. Health, 11A(6) (1976) 397.
15 C. C. Badcock, H. W. Sidebottom, J. G. Calvert, G. W. Reinhardt and E. K. Damon, J. Am. Chem. Soc., 93 (1971) 3115.
16 G. F. Jackson and J. G. Calvert, J. Am. Chem. Soc., 93 (1971) 2593.
17 H. W. Sidebottom, C. C. Badcock, J. G. Calvert, B. R. Rabe and E. K. Damon, J. Am. Chem. Soc., 93 (1971) 3121.
18 K. L. Demerjian, J. G. Calvert and D. L. Thorsell, Int. J. Chem. Kinet., 6 (1974) 829.
19 R. B. Timmons, Photochem. Photobiol., 12 (1970) 219.

20 F. C. James, T. A. Kerr and J. P. Simons, Chem. Phys. Lett., 25 (1974) 431.
21 R. D. Penzhorn and W. G. Filby, J. Photochem., 4 (1975) 91.
22 A. Horowitz and J. G. Calvert, Int. J. Chem. Kinet., 5 (1973) 243.
23 F. B. Wampler, A. Horowitz and J. G. Calvert, J. Am. Chem. Soc., 94 (1972) 5523.
24 F. B. Wampler, J. G. Calvert and E. K. Damon, Int. J. Chem. Kinet., 5 (1973) 107.
25 R. A. Cox, J. Photochem., 2 (1973) 1.
26 H. D. Mettee, J. Phys. Chem., 73 (1969) 1071.
27 H. W. Sidebottom, C. C. Badcock, G. E. Jackson, J. G. Calvert, G. W. Reinhardt and E. K. Damon, Environ. Sci. Technol., 6 (1972) 72.
28 R. P. Penzhorn and G. H. Gusten, Z. Naturforsch., 27a (1972) 1401.